Carcinogenesis, 2019, 1–13

doi:10.1093/carcin/bgz151
Advance Access publication August 31, 2019
Original Article

ORIGINAL ARTICLE

MKP1 phosphatase is recruited by CXCL12 in glioblastoma cells and plays a role in DNA strand breaks repair

Matthias Dedobbeleer[1,*], Estelle Willems[1], Jeremy Lambert[1], Arnaud Lombard[1,2], Marina Digregorio[1], Paul Noel Lumapat[1], Emmanuel Di Valentin[3], Stephen Freeman[1], Nicolas Goffart[4], Felix Scholtes[1,2] and Bernard Rogister[1,5]

[1]Laboratory of Nervous System Diseases and Therapy, GIGA-Neuroscience, University of Liège, Liège, Belgium, [2]Department of Neurosurgery, CHU of Liège, Liège, Belgium, [3]Viral Vector Platform, GIGA Institute, University of Liège, Liège, Belgium, [4]The T&P Bohnenn Laboratory for Neuro-Oncology, Department of Neurosurgery, UMC Utrecht, Utrecht, The Netherlands and [5]Department of Neurology, CHU of Liège, Liège, Belgium

*To whom correspondence should be addressed. Tel: +32 43665917; Fax: +32 43665912; Email: mdedobbeleer@alumni.uliege.be

Abstract

Glioblastoma (GBM) is the most frequent and aggressive primary tumor in the central nervous system. Previously, the secretion of CXCL12 in the brain subventricular zones has been shown to attract GBM cells and protect against irradiation. However, the exact molecular mechanism behind this radioprotection is still unknown. Here, we demonstrate that CXCL12 modulates the phosphorylation of MAP kinases and their regulator, the nuclear MAP kinase phosphatase 1 (MKP1). We further show that MKP1 is able to decrease GBM cell death and promote DNA repair after irradiation by regulating major apoptotic players, such as Jun-N-terminal kinase, and by stabilizing the DNA repair protein RAD51. Increases in MKP1 levels caused by different corticoid treatments should be reexamined for GBM patients, particularly during their radiotherapy sessions, in order to prevent or to delay the relapses of this tumor.

Introduction

Glioblastoma (GBM), a grade IV glioma (WHO), is one of the deadliest primary brain tumors in the central nervous system due to its aggressiveness, its high clinical, intra- and intercellular and molecular heterogeneity and its characteristic systematic relapses (1). In comparison with other solid tumors in the brain, GBM is largely disseminated in the brain parenchyma, which renders complete surgical resection complicated nay impossible. In addition, the concomitant radio-chemotherapy after surgery confers a slight rise in overall survival but cannot avoid patients' systematic relapses (2). Those relapses are caused either by cells left behind after surgery, or by cells resistant to these combined therapies. As some of these cells able to regrow tumors share common properties with neural stem cells (3), they have been named glioblastoma-initiating cells (GICs) (4). We have demonstrated previously that some GBM cells are able to migrate specifically from the tumor mass to the subventricular zone (SVZ) due to (i) an elevated production of the chemokine CXCL12 in this brain region, and (ii) the overexpression of the CXCR4 receptors by migrating GBM cells (5). We have also shown that the majority of GBM cells present in the SVZ are GICs, as they have a higher propensity to develop new tumors (3). Multiple therapeutic strategies have been created (6) to target them specifically, without any significant success. Finally, we have shown that GBM cells within the SVZ are radioprotected in this neurogenic niche due to high local CXCL12 concentrations (7). In parallel, numerous clinical publications have recently pointed out the impact of GBM contact to human SVZ in patient survival (8), in GBM recurrences (9,10), suggesting an

Received: June 21, 2019; **Revised:** August 10, 2019; **Accepted:** August 29, 2019

Abbreviations:

ERK	extracellular signal-regulated kinase
GBM	glioblastoma
GIC	glioblastoma-initiating cell
JNK	Jun-N-terminal kinase
MAPK	mitogen-activated protein kinase
MCL1	myeloid cell leukemia 1
MKP1	MAP kinase phosphatase 1
mRNA	messenger RNA
PARP1	poly (ADP-ribose) polymerase 1
Rembrandt	Repository of Molecular Brain Neoplasia Data
SVZ	subventricular zone
TCGA	The Cancer Genome Atlas
WT	wild-type

SVZ-induced radioprotection of GBM cells (11). At present, the impact of SVZ-specific irradiation is under investigation in order to evaluate its benefit to patients' survival (10,12,13).

The role of the chemokine CXCL12, produced in the SVZ by endothelial cells and astrocytes, could thus play a role in patient relapse, either by stimulating GBM cells to escape from the tumor mass and invade the brain tissue toward the SVZ, or by stimulating GBM cells' radioresistance. However, the molecular mechanism behind the CXCL12-dependant radioprotection of GBM cells remains elusive.

In this study, we highlight the role of the MAP kinase phosphatase 1 (MKP1) in GBM radioprotection. MKP1, which is encoded by *DUSP1*, is a dual specificity phosphatase able to dephosphorylate tyrosine or serine/threonine amino acids. MKP1 is known to be overexpressed in breast, lung or prostate cancer (14) and to modulate the control of immunity in macrophages cells (15). In GBM, its exact role remains unclear, but MKP1 seems to increase GBM resistance against current therapies (16) and promote GIC differentiation (17,18). We demonstrate here that the activation of CXCR4 receptor by CXCL12 causes an increase in the phosphorylation of MKP1, which stabilizes the protein. Phosphorylated MKP1 protects GBM cells against death after irradiation by lowering apoptosis through the inactivation of the mitogen-activated protein kinase Jun-N-terminal kinase (MAPK JNK) and the stabilization of myeloid cell leukemia 1 (MCL1). Furthermore, MKP1 also promotes enhanced DNA repair by promoting the recruitment and stabilization of DNA repair protein RAD51 at DNA breaks.

Material and methods

Cell culture

Human U87MG (certified by Bio-Synthesis, Lewisville, TX), GB138 and MD1 (wild-type (WT) p53, IDH non-mutated and O-6-methylguanine-DNA-methyltransferase non-methylated) cells were cultivated as described previously (3,19). Prior to CXCL12 addition (12.5 or 100 nM), U0126 (10 μM) or before irradiation, the cells were serum starved for 12 h. The characterization of all cell culture was performed and can be found in Supplementary Material and Methods, available at *Carcinogenesis* Online.

Lentiviral vectors

U87MG and MD1 cells were transduced following an established protocol and can be found in Supplementary Material and Methods, available at *Carcinogenesis* Online.

Phosphoproteome analysis

U87MG cells were stimulated for 1 h with 0 or 12.5 nM human recombinant CXCL12 (n = 3) (Peprotech®, London, UK), collected and analyzed by the posttranslational modifications scan direct for phosphorylation: Multipathway Reagent V2.0 (Cell Signaling Technology®, Leiden, the Netherlands). The significant relative fold change was established at ±2.5 (P value < 0.05).

Human tissue samples and immunohistochemistry

Human tissue samples and immunohistochemistry staining were provided and performed by the Bio-bank and the Histology platforms of the GIGA Institute (University of Liège). Frozen tissues were fixed with acetone (15 min at 4°C) and blocked with 3% H_2O_2 (15 min). The primary Anti-MKP1antibody (goat polyclonal 1:100, ab1351; Abcam) was incubated 1 h at room temperature and revealed with diaminobenzidene. Nuclei were colored with hematoxylin. The experiments were undertaken with the understanding and the written consent of each subject. The study methodologies conformed to the standards set by the Declaration of Helsinki and were approved by CHU Liège ethics committee.

Immunofluorescence microscopy

Immunofluorescence experiments were performed as described previously (5) and all antibodies as well as the microscope and the softwares used can be found in Supplementary Material and Methods, available at *Carcinogenesis* Online. Primary antibodies were diluted and incubated overnight in a 1% donkey serum and 0.3% triton X-100 phosphate-buffered saline solution. Cells were then washed three times in phosphate-buffered saline, incubated 1 h at room temperature with secondary antibodies and counterstained a Hoechst dye (Thermo Fischer Scientific®).

Western blot

Western blots (WBs) were performed as described previously (7) and all antibodies used can be found in Supplementary Material and Methods, available at *Carcinogenesis* Online. These primary antibodies were incubated overnight at 4°C. Secondary antibodies were incubated for 1 h at room temperature. All WB quantifications performed to compare different conditions were always present on the same gel/blot.

Comet assay

The comet assays were performed using OxiSelect™ Comet Assay kit (Cell Biolabs®). The complete protocol can be found in Supplementary Material and Methods, available at *Carcinogenesis* Online.

Clinical databases

Clinical data and messenger RNA (mRNA) expression level data were obtained from the Repository of Molecular Brain Neoplasia Data (Rembrandt, http://www.betastasis.com/glioma/rembrandt/) and The Cancer Genome Atlas (TCGA) Portal (https://portal.gdc.cancer.gov/). From the Rembrandt database (n = 524), *DUSP1* mRNA expression levels (from Affymetrix HG-U133 v2.0 Plus) were obtained from cohorts of GBM (n = 214), astrocytomas (n = 145), oligodendrogliomas (n = 66) and non-tumoral tissues (n = 21). From the TCGA database, a cohort of 438 primary GBM patients with complete data was extracted. *DUSP1* mRNA expression levels were extracted from Affymetrix HT HG-U133A, Affymetrix Human Exon 1 ST and custom-designed Agilent feature Gene Expression Microarrays, according to standard methodology protocol (20). The Kaplan–Meier curves were based on Rembrandt database and were obtained by dividing patients in two groups following their high or low *DUSP1* mRNA expression levels in the tumor sample.

Proliferation assays

GBM cells were plated at a density of 500 cells per well in a 6-well plate (Corning®), stimulated for 1 h with 100 nM CXCL12 (Peprotech®) and irradiated by the Gammacell® 40 Extractor with 0, 5 or 10 Gy (Best Theratronics®, Ottawa, Canada). The complete protocol can be found in Supplementary Material and Methods, available at *Carcinogenesis* Online.

Migration assays

Migration assays were performed as described previously (21) in 96-wells chemotactic chamber with 10 μm pore at a density of 10^3 pores per mm^2 (Neuro Probe Inc, Gaithersburg, MD). The complete protocol can be found in Supplementary Material and Methods, available at *Carcinogenesis* Online.

Statistical analyses

Quantitative data are expressed as mean ± SD/±SEM and analyzed by GraphPad Prism 7®. Student' t-test, two-way analysis of variance test and Tukey and Bartlett's posttests were used to analyze a minimum of three biological experiments (n = 3) and a P value of <0.05 was considered as statistically significant.

Results

Regulation of MAPK following CXCL12 stimulation in GBM cells

We demonstrated previously that both the migration of GBM cells (5) and their radioresistance (5,7) are triggered by CXCL12, but the exact molecular mechanisms behind these two different cellular responses is still unknown. To identify the specific pathways triggered, we performed a mass spectrometry analysis on protein extracts of U87MG cells, stimulated for 1 h by CXCL12 (12.5 nM) or not. We detected several proteins whose phosphorylation level was significantly changed (21). Among others, a higher phosphorylation profile of the MAPK extracellular signal-regulated kinase (ERK) (fold change: 3.6), the phosphatase MKP1 (fold change: 5.4) and a lower phosphorylation profile of the MAPK JNK (fold change: −15.2) were observed in CXCL12-stimulated cells compared with unstimulated cells (non-treated) (Figure 1A). The MAPK p38 phosphorylation profile was not significantly lowered (fold change: −1.4). The effectors of the MAP kinase pathway (Figure 1B) were thus modulated upon the binding of the chemokine CXCL12 on its receptors.

These results were confirmed in WBs on protein extracts of U87MG cells and three primary GBM cultures, GB138, MD1 and MD18, in response to a CXCL12 stimulation (12 5 nM) (Figure 1C–G and Supplementary Figure 1A and B, available at *Carcinogenesis* Online). For the phosphatase MKP1 and kinase ERK, phosphorylation increased after 15 min in all cell cultures. Contrary to GB138 cells, where the phosphorylation peak of MKP1 was reached after 30 min, in U87MG cells and in primary MD1 and MD18 cells, MKP1's phosphorylation increased to its maximum after 60 min. It is interesting to note here that the increased phosphorylation of MKP1 is linked with an increase of its total form. The phosphorylation profile of the MAPK JNK was the same in all cultures with an increasing phosphorylation up until 30 min, followed by a significant decrease after 60 min. Regarding the MAPK p38, the phosphorylation profile was largely unchanged until a slight but not significant decrease after 60 min of CXCL12 stimulation.

CXCL12 is known to activate two different receptors, CXCR4 and CXCR7, which are expressed at different levels in GBM (21) (Supplementary Figure 1C, available at *Carcinogenesis* Online). In order to evaluate the potential effect of CXCR7, we pretreated the three different GBM cell cultures with the specific inhibitor of the CXCR4 receptor AMD3100 (22) prior to CXCL12 addition. CXCR4 inhibition led to a lower phosphorylation profile of MKP1 in GB138 and MD1 cells, contrary to JNK, which showed a higher phosphorylation profile in all GBM cell cultures (Supplementary Figure 1D and E, available at *Carcinogenesis* Online). ERK phosphorylation was also increased after CXCL12 stimulation in GB138 and in MD1 cells compared with unstimulated cells (non-treated), but not in U87MG cells. MAPK p38 phosphorylation remained unchanged (Supplementary Figure 1D and E, available at *Carcinogenesis* Online). This suggests that the recruitment of the phosphatase MKP1 and the inhibition one of its preferential targets (23), JNK, are closely related to the activation of CXCR4 in GBM cells.

Finally, we wanted to evaluate if the recruitment of the MAP kinase ERK had an impact on the phosphorylation of other MAP kinases. Indeed, serine phosphorylation of MKP1 after CXCL12 is generally believed to be under ERK control. Inhibition of the ERK pathway *via* pretreatment with the inhibitor U0126 1 h prior to CXCL12 stimulation decreased the phosphorylation of MKP1 (Supplementary Figure 1F, available at *Carcinogenesis* Online) in U87MG and MD1 cells. In addition, an increased phosphorylation of JNK was also observed in these two cell types under the same conditions. P38 phosphorylation was unchanged.

Expression of MKP1 in GBM cells

Because MKP1 is highly phosphorylated in GBM cells in response to a CXCL12 stimulation, alongside its overexpression in various cancers (14) and its implication in multiple physiopathological states including inflammation or obesity (24), we decided to focus our attention on this phosphatase. We first checked its expression profile in the human databases Rembrandt and TCGA. In the Rembrandt database, we identified higher expression levels of MKP1 in GBM samples compared with non-tumoral brain tissues, but this increase was not statistically significant (P = 0 0657) (Figure 2A). In order to confirm this increased expression of MKP1 in GBM tissues, we performed immunostainings for this phosphatase on GBM samples obtained from the clinic (Figure 2C, right panel), and brain tissues obtained from epileptic patients (Figure 2C, left panel). Staining quantification showed that the expression of MKP1 was significantly increased in GBM samples compared with non-tumoral tissues (Figure 2D). By comparing the different subtypes of GBM, based on Verhaak's classification (20) in the TCGA database, we observed significantly higher expression levels of MKP1 in the mesenchymal subtype (P = 0.0001) (Figure 2B), a subtype associated with a poor prognosis. Using data from the Rembrandt database on GBM patient survival and the expression of MKP1, we found that patients for whom MKP1 expression was downregulated had a better significant survival compared with patients whose tumors express this protein at high levels (Figure 2E).

The expression of the gene (Figure 2F) and its protein (Figure 2G) were then analyzed in different cultivated GBM cell cultures by Reverse Transcriptase PCR and WB, respectively. MKP1 is classified as a nuclear phosphatase because of the nuclear localization signal (25), which distinguishes it from the other member of the MAP kinase phosphatases. As expected, immunostaining of the protein confirmed that MKP1 is predominantly present in the nuclei of the cells (Figure 2H).

Finally, given the importance of both CXCR4 and CXCR7 in GBM (26,27) and CXCR4 as marker of GIC (28), we cross-referenced the expression of their respective genes with the expression of MKP1 in the TCGA database. The results showed a significant correlation (r = 0.5654) between the expression of MKP1 and CXCR4 (Figure 2I) compared with CXCR7 (r = −0.1380) (Figure 2J). This supports our data in which the inhibition of CXCR4 in cells stimulated by CXCL12 was not followed by an increased phosphorylation of MKP1 (Figure 1D and E).

As the expression profile of MKP1 in the primary culture GB138 cells and its pathways are regulated differentially in response to CXCL12 stimulation, we decided to focus our attention on U87MG and MD1 cells.

Role of MKP1 inhibition on GBM cells migration

As mentioned previously, CXCL12 stimulates the GBM cell migration (5) and promotes their radioresistance (7). In order to study the possible involvement of MKP1 in GBM cell migration, different

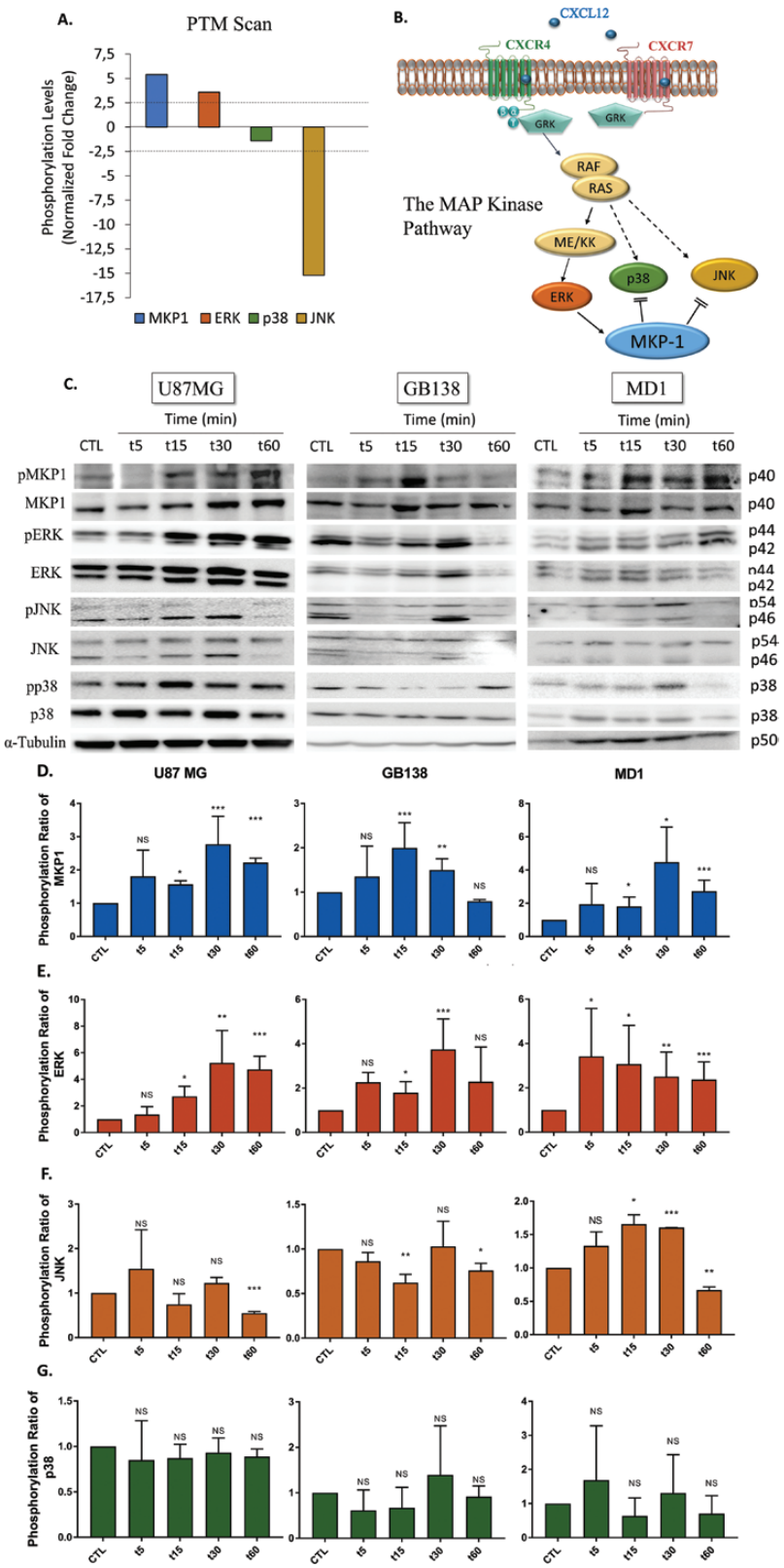

Figure 1. Activation of the MAPK pathway following CXCL12 treatment in GBM cells. (**A**) Bar graph presenting results of the phosphoproteome profile analysis of various proteins of the MAPK pathway whose phosphorylation is modified in U87MG cells after 1 h of CXCL12 stimulation (12 5 nM) or not. The graph shows the phosphorylation fold change for MKP1, ERK, JNK and p38 in protein extracted from U87MG cells stimulated during 1 h with CXCL12 compared with unstimulated cells. (**B**) Diagram presenting the different proteins of the MAP kinase pathway whose phosphorylation profile changes after CXCL12 docking on one of its receptor, CXCR4. (**C**) WB analysis and quantification of P-MKP1 (**D**), P-ERK (**E**), P-JNK (**F**) and P-p38 (**G**) in proteins extracted from respectively U87MG, GB138 and MD1 cells non-treated (NT) or stimulated for 5, 15, 30 and 60 min with CXCL12 (12 5 nM). Graphs are mean values ± SEM and are representative of three independent experiments, *P <0.05, **P <0.01, ***P <0.001 (two-way analysis of variance).

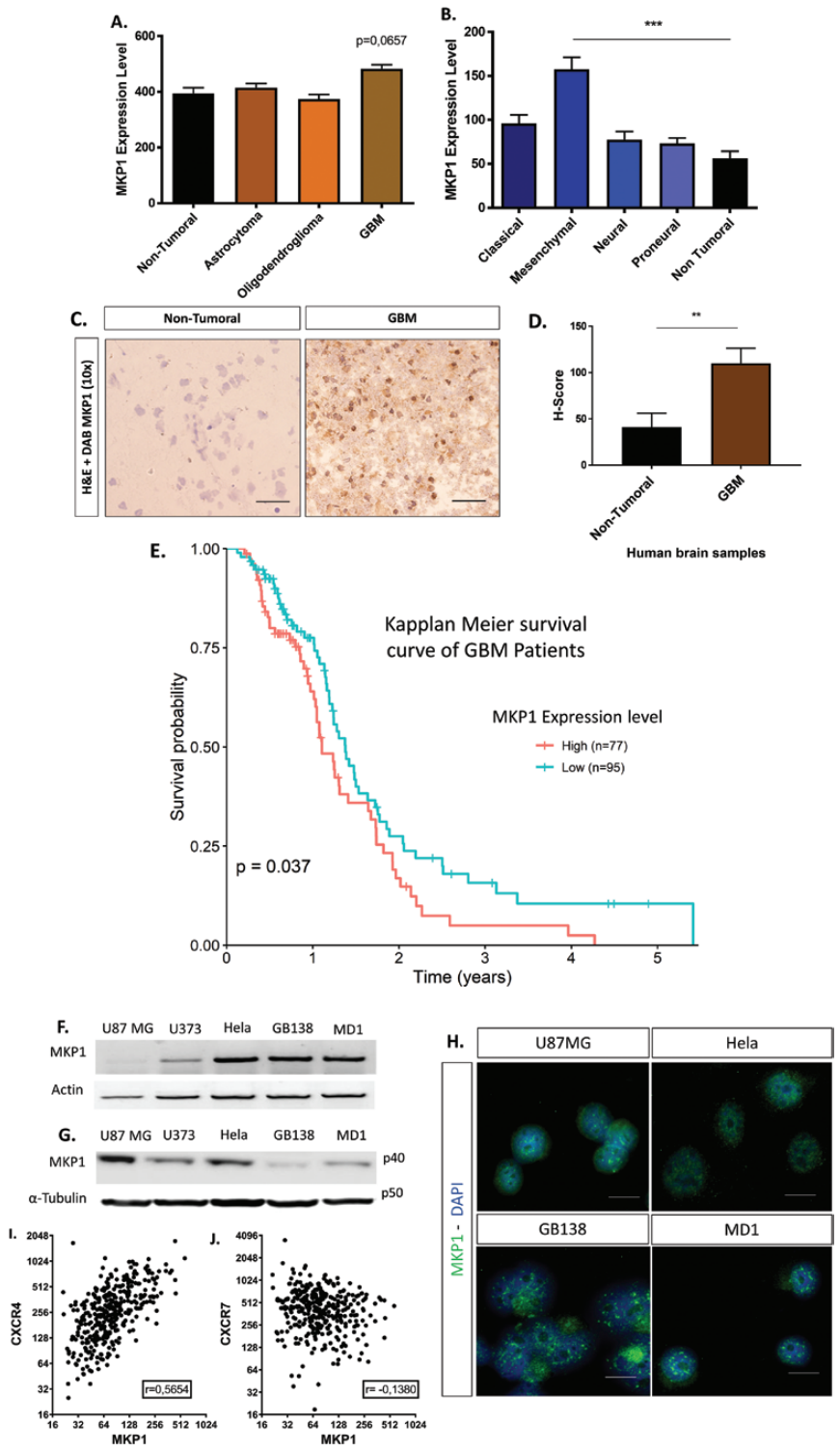

Figure 2. Expression of MKP1 in GBM cells. (**A**) Rembrandt data for *DUSP1* (MKP1 encoding gene) mRNA expression in arbitrary units in human non-tumoral brain tissues ($n = 21$), astrocytomas ($n = 145$), oligodendrocytomas ($n = 66$) and GBM samples ($n = 214$). (**B**) TCGA data for MKP1 mRNA expression in arbitrary units in non-tumoral brain tissues and in different GBM subtypes (classical, mesenchymal, neural and proneural). (**C**) Kaplan–Meier curve presenting three groups of GBM patients' survival (in months) upon the expression of MKP1 (low <–2 in blue, intermediate in yellow and high >2 in red). (**D**) Immunohistology staining of MKP1 (DAB) in human non-cancerous (i.e. temporal lobe from epileptic patient) ($n = 3$) and GBM ($n = 3$) tissues (H&E staining, ×10). The lower panels show GBM tissue at ×40 magnification. (**E**) The graph shows the mean intensity of MKP1 staining by DAB in non-cancerous and GBM tissues quantified by Image J software. Scale bars = 100 µm. Graphs are mean values ± SD and are representative of three independent experiments, $^{*}P < 0.05$, $^{**}P < 0.01$, $^{***}P < 0.001$ (t-test corrected by posttests) (**F**) Terminal Reverse Transcriptase PCR analyses and (**G**) WB analysis of MKP1 expression in respectively total RNA or proteins extracted from U87MG and U373 cells, GB138 and MD1 primary cultures and Hela cells used as a positive control. (**H**) Immunocytofluorescent staining of MKP1 in U87MG cells, GB138 and MD1 primary cultures, and Hela cells used as control (scale bar = 10 µm). (**I**) Correlation analyses between the expression of MKP1 and the receptors CXCR4 and (**J**) CXCR7. Pearson's correlation coefficient (r): correlation high (>0.5), small (between 0.5 and 0); non-correlated (close to 0); inverse correlation small (between 0 and –0.5), high (>–0.5). DAB, diaminobenzidene; H&E, Hematoxylin and Eosin.

short-hairpin RNAs (shRNAs) targeting MKP1 expression were tested in U87MG cells. We selected the sh1489 that showed a depletion of MKP1 protein by 75% compared with the effect of a scrambled shRNA (Figure 3A). sh1489 inhibition of MKP1 expression in primary culture cells GB138 and MD1 also produced similar levels of MKP1 expression inhibition (Supplementary Figure 2A and C, available at *Carcinogenesis* Online). In order to evaluate the effects of the opposite situation, we transfected the U87MG cells with an OverExpression (OE) plasmid (pGIII) (Figure 3B). Transduction of the MKP1 plasmid for its overexpression in primary cultures was also performed showing the similar results (Supplementary Figure 2B and D, available at *Carcinogenesis* Online). A quantification of MKP1 expression between all control cells was performed in order to confirm that MKP1 expression remained stable (Figure 3C) (Supplementary Figure 2E and F, available at *Carcinogenesis* Online).

We first addressed the question of whether if MKP1 downregulation had an impact on the phosphorylation of other MAP kinases. By stimulating shMKP1-transfected U87MG and MD1 cells with the chemokine CXCL12, we were able to conclude that the phosphatase was only targeting the MAP kinase JNK, as its phosphorylation increased after 1 h of stimulation (Figure 3D). The profile of the other MAP kinases remained unchanged and the profiles obtained in the control cells (sheGFP) (Supplementary Figure 2G, available at *Carcinogenesis* Online) reproduced the profiles obtained previously (Figure 1).

Knowing that the chemokine CXCL12 is known to be responsible for GBM cells enhanced migration (5), we performed a migration assay based on the modified Boyden chambers assay. We could not see any differences in the migration profile when cells were depleted for MKP1 after 16 h of CXCL12 stimulation, which was added in the bottom chambers (Figure 3E and F).

Role of MKP1 on GBM cells survival after irradiation

Previous studies have shown that the environment of the SVZ can radioprotect human GBM cells *via*, at least partly, the chemokine CXCL12 (7). As MKP1 has already been implicated in radioprotection in other cancers (29,30), we performed clonogenic assays using GBM cells invalidated for or overexpressing MKP1 and stimulated (or not) with CXCL12 (100 nM) for 1 h before irradiation. The cells were then irradiated with 0, 5 and 10 Gy (Figure 4A). The survival fraction of shMKP1 cells (calculated from the numbers of colonies formed 2 weeks after irradiation) was significantly lower than the survival fraction observed with GBM cells with a basal or a stimulated expression of MKP1 without any exogenous CXCL12 stimulation (Figure 4A, left panels). Surprisingly, the addition of chemokine CXCL12 (100 nM) in the medium was not followed by dramatic changes in the survival profile of the cells (Figure 4A, right panels). Nevertheless, after a stimulation by CXCL12, MKP1 depletion still diminished the survival of all GBM cells after a 10 Gy irradiation. However, by comparing results obtained with or without CXCL12 addition, a significant survival increase was observed in U87MG and MD1 cells showing at least a basal expression of MKP1 whereas the chemokine did not increase the GBM cells survival when MKP1 expression had been invalidated (Figure 4B). Taken together, these results highlight the role of MKP1 in GBM cells survival after irradiation, which was boosted by the addition of CXCL12, a chemokine shown previously to be able to recruit MKP1 (Figure 1).

In order to confirm these results, comet assays were performed to assess the possible effect of MKP1 depletion on DNA strand breaks repair. The analysis of comet tails revealed that shMKP1 cells had a significant higher percentage of DNA in the tail (close to 40%) compared with cells with a basal or higher MKP1 expression (Figure 4C and D). The addition of the chemokine CXCL12 did not show any effect on the percentage of DNA in the tail, indicating that the chemokine did not have, in this time frame, a positive effect upon DNA strand break repair in any of the tested GBM cells. However, the positive effect of MKP1 on DNA strand break repair was still observed when CXCL12 has been added previously.

The comet assay highlighted here the major role of MKP1 as a modulator of DNA strand breaks repair in GBM cells and thus possibly increasing their capacity for survival after irradiation.

Time course of markers of DNA strand breaks in GBM cells after irradiation upon MKP1 inhibition

We then tried to elucidate the exact mechanism(s) behind the involvement of MKP1 in DNA strand repair in GBM cells. For this purpose, we quantified the number of DNA double strand breaks at time intervals up to 24 h after 10 Gy irradiation in GBM cells. This was done by counting the number of phosphorylated H2AX foci (or γH2AX), which specifically marks DNA damage such as strand breaks. Interestingly, in all GBM cell cultures, the depletion of MKP1 significantly increased the number of foci per nuclei before the irradiation (non-irradiated conditions) (Figure 5A and B). After irradiation, a significantly higher number of γH2AX foci per cell nuclei were observed in U87MG and MD1 cells (Figure 5A and B). These results could suggest that the absence of MKP1, or reduced MKP1 activity, in U87MG or MD1 cells is linked to higher number of DNA double strand breaks in the presence or absence of irradiation. 24 h after irradiation, the number of γH2AX foci per cell nuclei decreased when MKP1 is absent. However, a lower number of cells were counted in this particular condition, suggesting that a reduced number of cells survived the DNA strand breaks. It is interesting to notice that in those two cell types, CXCL12 is able to increase cell survival (Figure 4B).

Therefore, we looked for a difference in the presence of DNA repair proteins in these two cell types in the presence and absence of MKP1 expression. The immunolabeling of RAD51, a protein implicated in homologous repair of DNA double strand breaks and cell cycle changes in GBM stem cells during S/G_2 phase of the cell cycle (31), revealed that cells invalidated for MKP1 expression recruited RAD51 at the break with a significant delay at 8 and 12 h after the irradiation irrespective of the GBM cell type (Figure 5C and D).

Role of MKP1 in apoptotic GBM cell death after irradiation

MKP1 is thus involved not just in the double strand break repair mechanism but also in GBM cell survival. To elucidate the potential connections between these cellular activities, we analyzed the evolving response of several molecular targets which are already known to interact with or could be a substrate of MKP1, specifically after irradiation, which could play a role in DNA strand breaks repair and/or in cell survival.

First, we looked for the expression of MKP1 itself by WB with or without irradiation. It was observed that MKP1 expression was significantly increased in response to irradiation, mainly at 6 and 8 h in all WT GBM cell types (Figure 6A and B). In GBM cells invalidated for MKP1 (shMKP1), only a faint increase in MKP1 expression 4 h after irradiation was observed.

As a potential target of MKP1 phosphatase, we investigated the phosphorylation profile of the MAP kinase JNK. As expected, its phosphorylation was significantly increased after irradiation in all shMKP1 GBM cells compared with WT cells (Figure 6A and

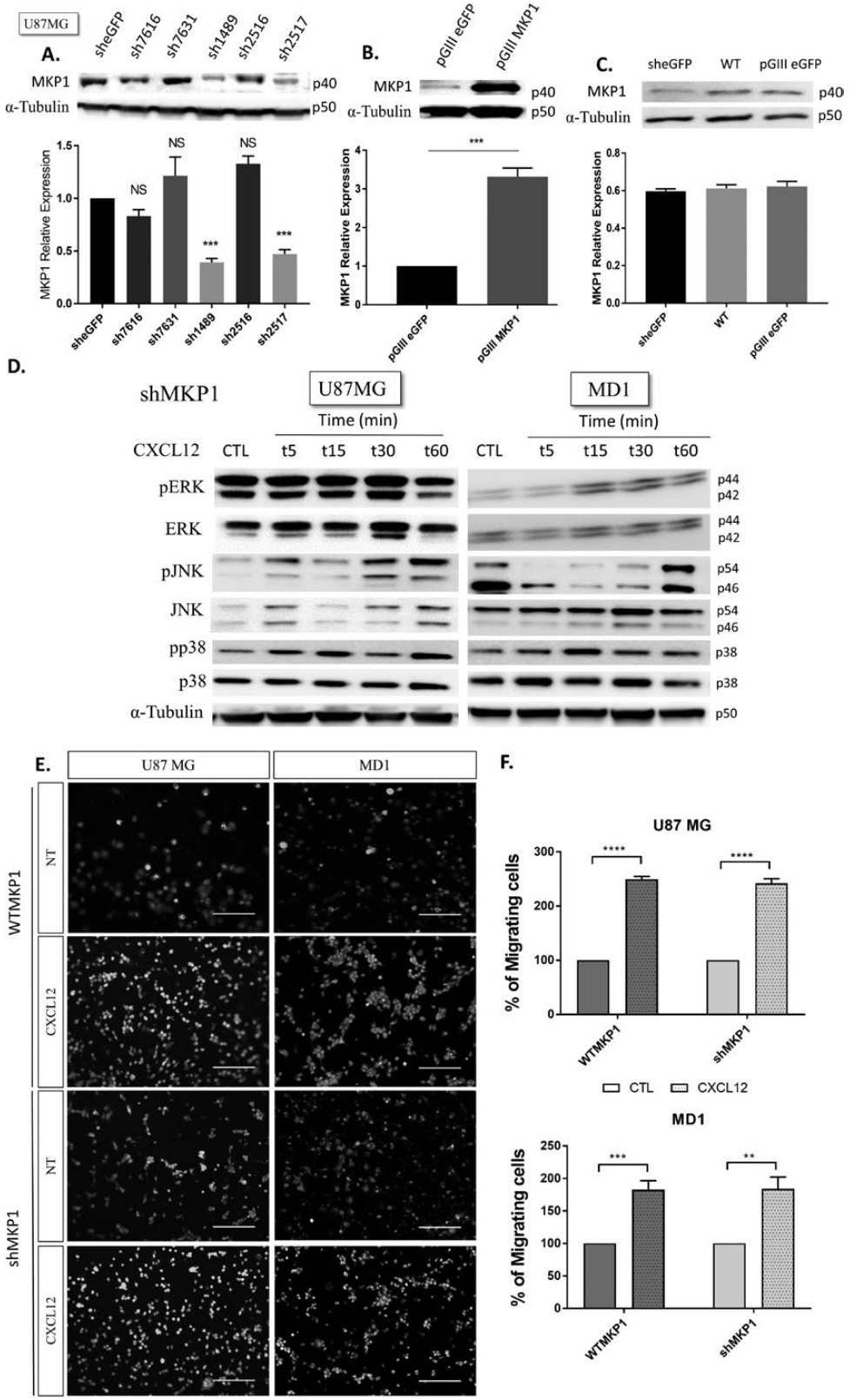

Figure 3. Evaluation of a possible MKP1 role in GBM cells migration and its modulation on other MAPK in response to CXCL12. (**A**) WB analysis of MKP1 expression in U87MG cells after transfection by different shRNA with the most efficient one (sh1489) decreasing the expression of MKP1 by 75% comparing with the MKP1 expression by cells transfected with a shRNA targeting enhanced green fluorescent protein (eGFP). (**B**) U87MG cells were also transfected with an expression plasmid allowing a MKP1 overexpression (U87MG pGIII MKP1). (**C**) Comparison of MKP1 expression by WB between all the control cells. (**D**) Analysis of ERK, JNK and p38 phosphorylation profiles by WB with extracts from U87MG and MD1 cells (shMKP1) treated with the CXCL12 (12.5 nM) or not (control) during 1 h. (**E**) Boyden's chamber migration assays using U87MG and MD1 cells (WT and shMKP1) treated with the CXCL12 (500 nM) or not (control) during 16 h. (scale bar = 20 µm). (**F**) Cell counting in the migration assays. For an easier understanding, the cells depleted for MKP1 will be called '*sh*MKP1' and the cells with a basal expression of MKP1 will be called '*WT*'. Graphs are mean values ± SEM and are representative of three independent experiments, $^{**}P < 0.01$, $^{***}P < 0.001$ (two-way analysis of variance).

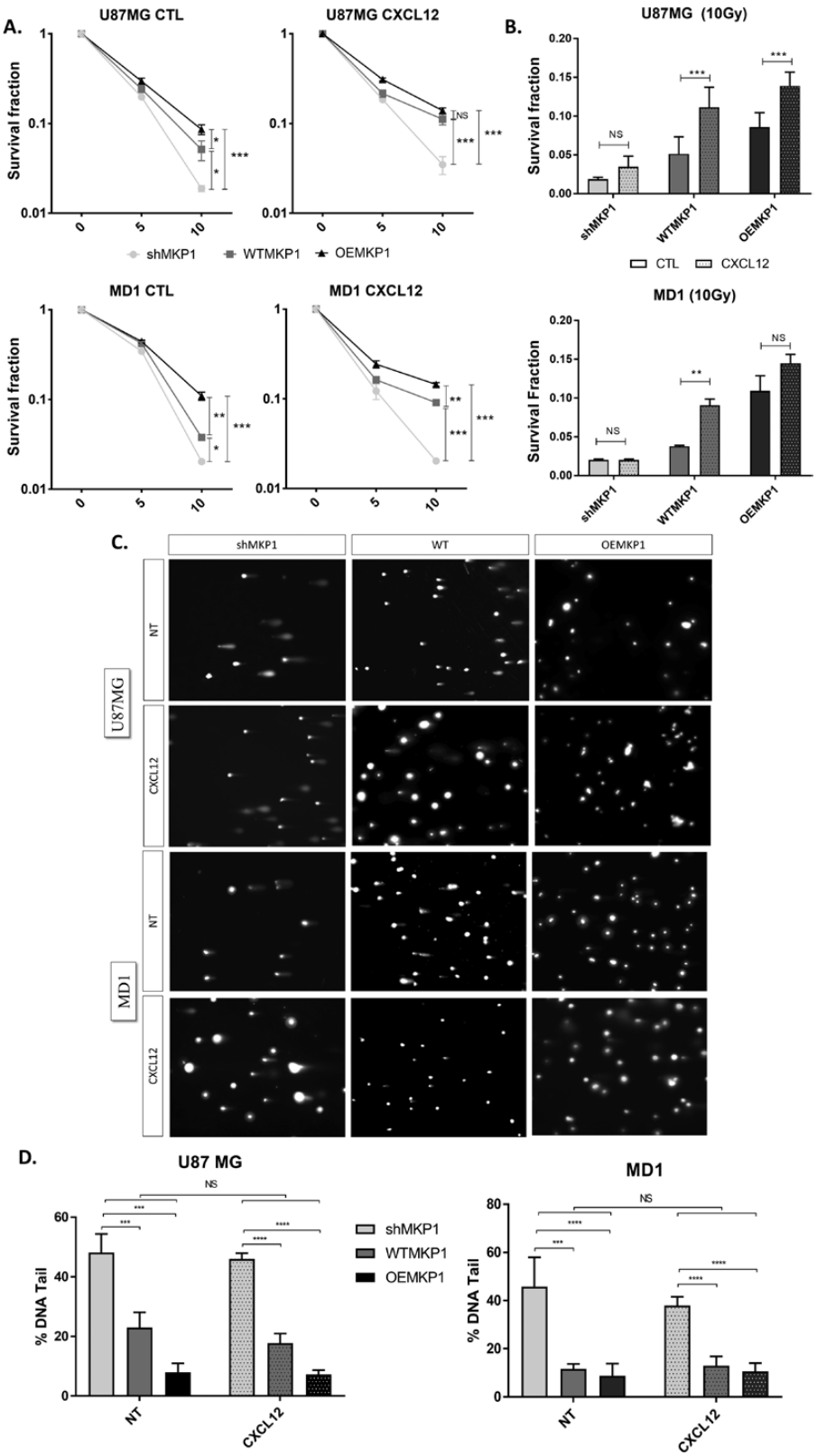

Figure 4. Positive effect of MKP1 in GBM cells DNA strand break repair. (**A**) This graph presents the survival fraction of U87MG and MD1 GBM cells invalidated, expressing or overexpressing MKP1 (named respectively shMKP1, WTMKP1 or OEMKP1) cells 2 weeks after 0, 5 or 10 Gy irradiation, and pretreated during 1 h by CXCL12 (100 nM) (right panels) or not (control) (left panels). (**B**) Graph presenting the comparison between the survival of GBM cells following MKP1 expression and CXCL12 stimulation (**C**) Figures presenting the comet assays of U87MG and MD1 GBM cells, invalidated, expressing or overexpressing MKP1 (named respectively shMKP1, WT or OEMKP1) 24 h after 10 Gy irradiation, stimulated by CXCL12 (100 nM) or not (no-treated, NT) (**D**) and graphs presenting tail DNA percentage (or DNA still fragmented). Graphs are mean values ± SEM and are representative of three independent experiments, **P* <0.05, ***P* <0.01, ****P* <0.001 (two-way analysis of variance). NS: not significant.

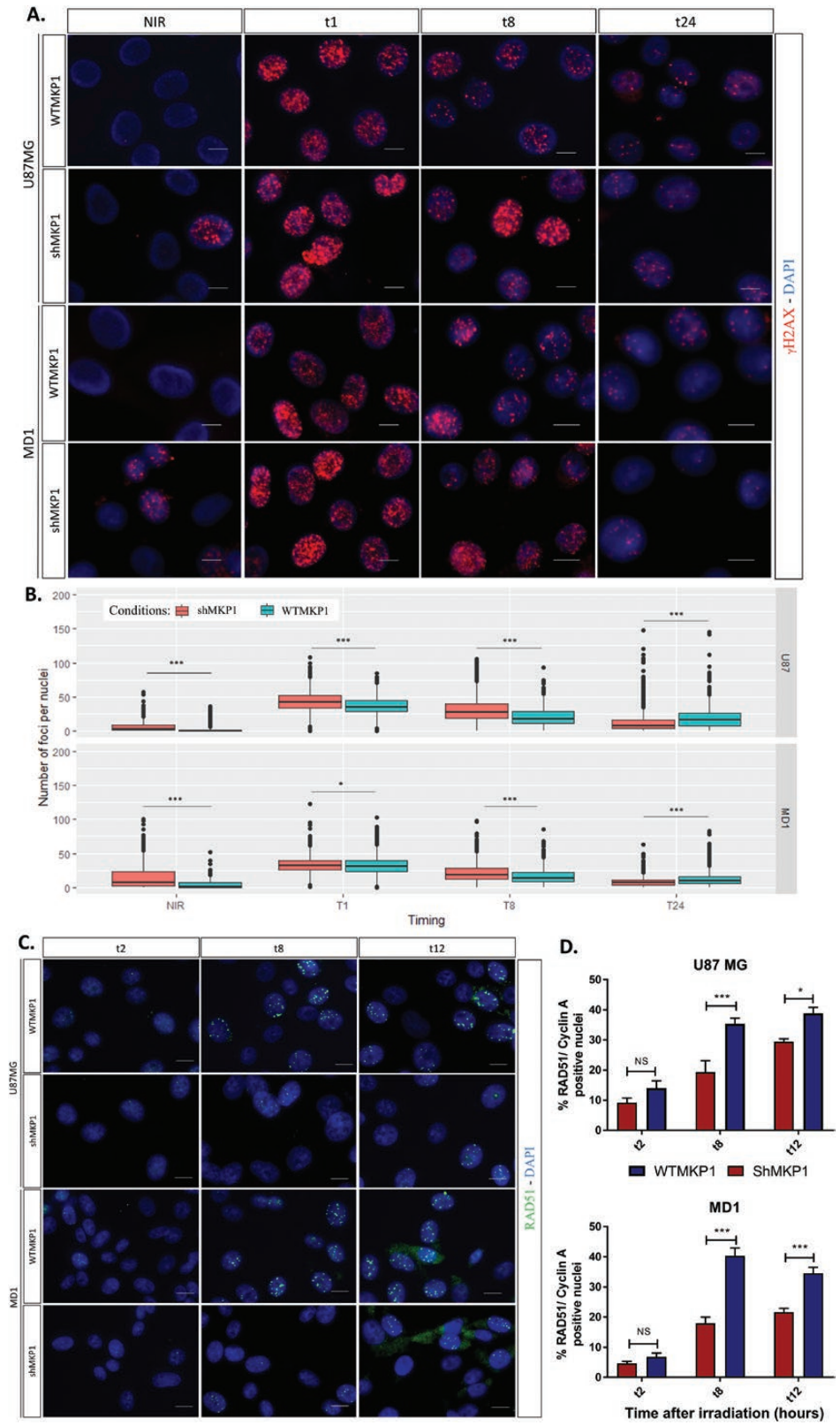

Figure 5. Consequences of MKP1 invalidation in GBM cells on DNA strand breaks and repair proteins. (**A**) Representative microphotographs presenting the labeling of γH2AX in U87MG and MD1 GBM cells invalidated or not for MKP1 (respectively, shMKP1 or WT) with their respective quantification below (**B**) (scale bar = 5 µm). These microphotographs have been captured in non-irradiated cells (NIR) cultures or in cultures 1, 8 and 24 h after the irradiation. (**C**) Representative microphotographs presenting the immunolabeling of nuclear RAD51 and cyclin A in U87MG and MD1 GBM cells invalidated or not for MKP1 (respectively, shMKP1 or WTMKP1) 2, 8 and 12 h after the irradiation with their respective quantification on the right (**D**) (scale bar = 5 µm). Graphs are mean values ± SEM and are representative of three independent experiments, * $P<0.05$, ** $P<0.01$, *** $P<0.001$ (two-way analysis of variance). NS: not significant.

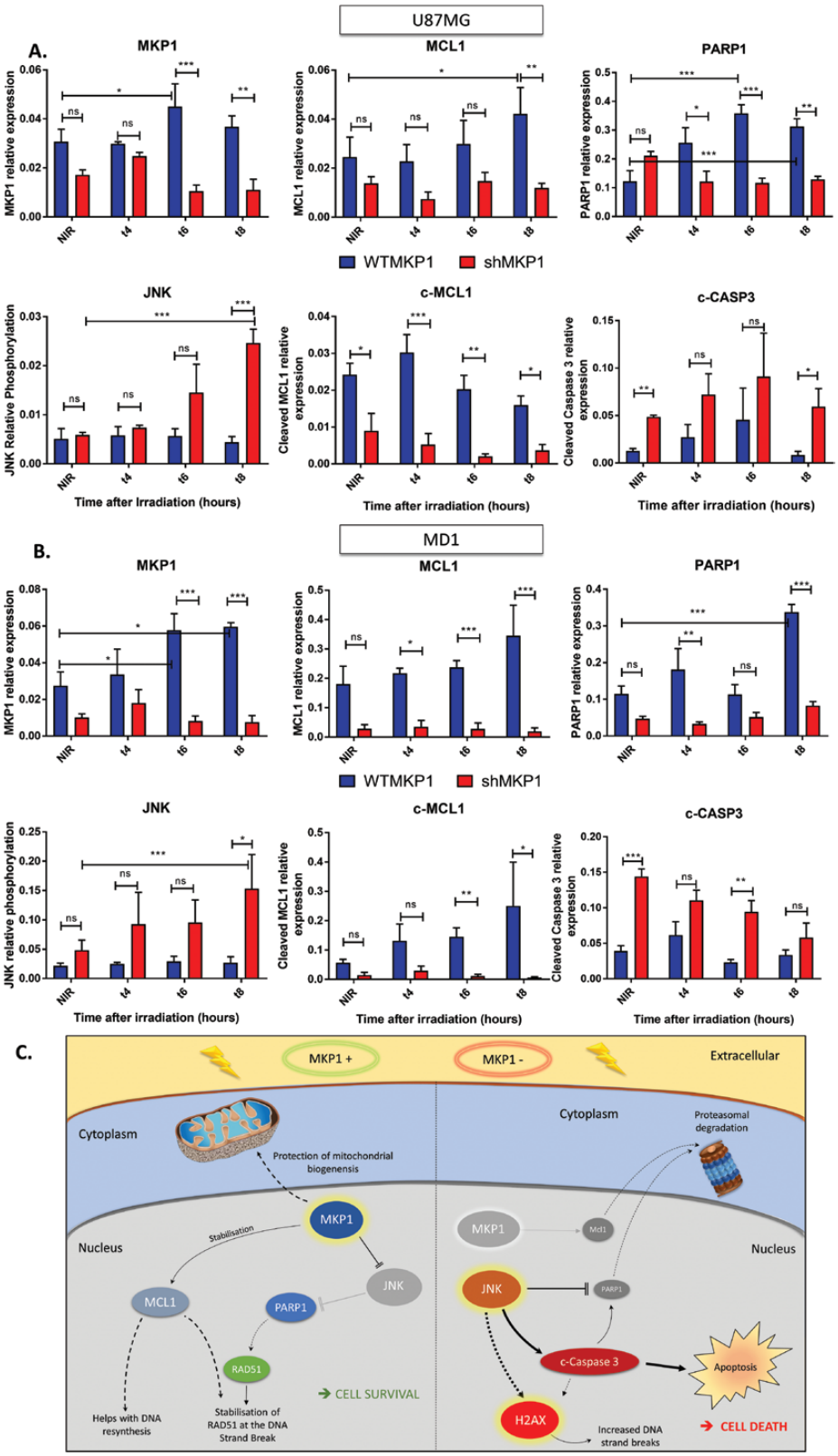

Figure 6. Effects of MKP1 depletion on downstream proteins playing a role in GBM cell survival. Graphs presenting the time evolution analyzed by WB of MKP1 expression, JNK phosphorylation and the expression of PARP1, MCL1 and the cleaved form of MCL1 and Caspase-3 in U87MG (**A**) and MD1 GBM cells (**B**) invalidated for MKP1 expression or not (respectively, shMKP1 in red and WT in blue) before (NIR) or 4, 6 and 8 h after irradiation. Graphs are mean values ± SEM and are representative of three independent experiments of WB on proteins extracted from U87MG or MD1 cells in various conditions, *P <0.05, **P <0.01, ***P <0.001 (two-way analysis of variance). (**C**) Diagram presenting the different pathways implicated after GBM cells irradiation when MKP1 is present (left side) or absent (right side). Black arrows represent a positive link, black space arrows a potential other link, gray arrows an inactive link and double black arrows an inhibition. MKP1, JNK and H2AX are surrounded with a yellow shadow when the protein is active and in gray with a white shadow when the protein is absent or inactive.

B). As JNK is more associated with modulating cell survival than DNA repair, the profile of one of its targets in cell survival, the poly (ADP-ribose) polymerase 1 (PARP1), was investigated. PARP1 is known to play a major role in DNA repair via the stabilization of breast cancer type 1 (BRCA1) which recruits RAD51 to the break (32). Although the total amount of PARP1 increased with time after irradiation in WT cells (but with differences in the timing between various GBM cell types), its level was significantly decreased in shMKP1 cells (Figure 6A and B).

MCL1 has been shown to play a role in the inhibition of GBM cell apoptosis (33) by controlling cytochrome C release from mitochondria (34). It can also increase GBM cell survival after bortezomib treatment (35). As recently highlighted, MCL1 is tightly regulated by MKP1 under stress conditions (Jagannathan,V. *The Phosphatase MKP1 as a Target to Enhance Replicative Stress and Apoptosis in Tumor Cells*. Ph.D. Thesis, unpublished work) and participates in DNA repair (36). We found that the total amount of MCL1 was not decreased by irradiation in WT cells (Figure 6A and B), but was significantly increased in U87MG cells in those conditions. The total form of MCL1 was significantly decreased in shMKP1 cells for all GBM cell types (Figure 6A and B), and moreover, the presence of a cleaved form of MCL1 (c-MCL1) (28 kD) was also observed to be stabilized after the irradiation in WT cells(Figure 6A and B), contrary to shMKP1 cells where this spliced form was absent.

Finally, we checked the cleavage of the caspase-3. In WT cells, caspase-3 was slightly cleaved compared with shMKP1 cells where its cleavage was significantly higher (Figure 6A and B).

To confirm all the results obtained and the specific link between MKP1 and JNK, we decided to rescue MKP1 expression in shMKP1 cell by overexpression of MKP1 in all GBM cultures used (Supplementary Figure 3A and B, available at *Carcinogenesis* Online). MKP1 rescue in shMKP1-U87MG line and -GB138 and -MD1 primary cultures stimulated for 1 h with CXCL12 (12 5 nM) significantly decreased the phosphorylation of JNK (Supplementary Figure 3C, available at *Carcinogenesis* Online). In addition, this rescue of MKP1 in shMKP1-U87MG and -MD1 cells significantly decreased JNK phosphorylation and increased the expression PARP1 and MCL1 as well as its cleaved form c-MCL1 8 h after irradiation (10 Gy) (Supplementary Figure 3D and E, available at *Carcinogenesis* Online).

Discussion

At present, an increasing number of observations point out the role of the SVZ in tumor relapses. Several clinical studies have reported that tumors contacting the SVZ correlate with lower patient survival rate (8,9). We have shown previously that GBM cells which migrate to this specific environment in a CXCL12-dependent manner are mainly GIC (5,7) GICs are increasingly believed to be responsible for, or at least to actively play a role in, tumors relapses (3). The phosphoproteome and WB analyses of U87MG cells stimulated for 1 h by CXCL12 identified a higher phosphorylation of the MAP kinase ERK and the nuclear phosphatase MKP1 in contrast to a lower phosphorylation profile of the MAP kinase JNK. Those results were confirmed using a GBM cell culture derived from a GBM resection piece obtained in the neurosurgical department of our academic hospital. In addition, the inhibition of ERK MAP kinase with U0126 enabled us to conclude that MKP1 becomes stabilized by ERK after CXCL12 stimulation, but also that MKP1 can dephosphorylate the MAP kinase JNK in GBM cells. A similar conclusion was reached when we showed that CXCL12 stimulation of shMKP1 cells increased JNK phosphorylation.

The main purpose of this study is to further clarify the role of MKP1 in GBM. The fact that this nuclear dual specificity phosphatase is overexpressed in GBM cells with a mesenchymal profile, one of the most aggressive subtypes (37), could be considered as a clue to its importance in GBM. In addition, patients harboring a tumor where MKP1 is expressed at higher levels have lower survival rate. However, in GBM stem cells, MKP1 has been reported to be downregulated (18), whereas its role, as an overexpressed pro-oncogenic protein, has already been highlighted in other solid tumors (14). Even if MKP1, with a lower basal expression, does not seems to be of major importance in GBM stem cells, the upregulation of this protein under stressful conditions in GBM cells could be significant. Indeed, as recently published by Stanzani *et al.* (38), irradiation of GBM stem cells promotes short-term expression of pro-inflammatory genes and a proneural to mesenchymal subtype switch.

As MKP1 is phosphorylated in GBM cells in response to a CXCL12 stimulation, and as CXCL12 is involved in GBM cell migration to the SVZ (5), we address the possible role of the phosphatase in the migratory response of GBM cells. However, our results clearly demonstrate the absence of this phosphatase recruitment in the migratory response of GBM cells to a CXCL12 stimulation. As another role of CXCL12 is the promotion of GBM cells radioresistance (7), we performed clonogenic and comet assays using cells invalidated or overexpressing MKP1. These results further clarified the role of MKP1 in GBM radioresistance. Indeed, the survival of the cells 2 weeks after irradiation as measured with the clonogenic assay was clearly increased when MKP1 was present (WT cells) or overexpressed (OEMKP1 cells) compared with cells depleted for MKP1. However, the addition of CXCL12 only had positive effects on U87MG and MD1 cell survival showing a basal (or stimulated, upon CXCL12 addition) MKP1 expression. shMKP1 or OEMKP1 cells, with lower levels of MKP1 expression, did not exhibit increases in cell survival after irradiation. These results indicate that MKP1 is important in GBM cell survival after irradiation, an important role which is exacerbated upon the addition of the chemokine CXCL12. These results were corroborated by comet assays showing a significant decrease of DNA strand breaks after irradiation in MKP1-expressing cells, regardless of GBM cell types. These results clearly demonstrated that MKP1 does play a role in GBM cells radioprotection by decreasing strand breaks induced by irradiation and, therefore, influences GBM cell survival.

Analysis of DNA damage through investigating the phosphorylation of H2AX histone has been used for many years. Indeed, this protein is known to fix directly to DNA double strand breaks and served as one of the first markers of this type of DNA damage. We reported previously that CXCL12 decreases the number of GBM cells positive for γH2AX 1 h after irradiation (7). However, comet assays performed 24 h after irradiation do not confirm a suspected radioprotective role of this chemokine. Therefore, we measured the γH2AX response in two GBM cell types for longer time periods. As we observed a difference in the number of γH2AX positive cells, we decided to count the number of foci per nuclei. The observation that all GBM cells depleted for MKP1 show a higher number of γH2AX foci strongly highlights the role of MKP1 in DNA strand break repair. This may be explained by the fact that the cells were cultivated in serum-free conditions, a stress sufficient to activate cleavage of caspase-3 and modify their cell cycle leading to strand breaks not being properly repaired without MKP1.

In irradiated U87MG and MD1 cells, the tendency for lower levels of DNA strand breaks repair when MKP1 is absent is confirmed a few hours after irradiation. In the two GBM cell types

(U87MG and MD1 cells), 24 h after irradiation, a lower number of foci were observed when MKP1 was absent. One potential explanation for this could be that the GBM cells unable to repair their DNA strand breaks have already undergone cell death and consequently, the mean number of foci per surviving cell is decreased. Alternatively, this could be explained by the fact that the phosphorylation of H2AX is consequence of DNA strand breaks but its dephosphorylation do not necessarily indicate repair.

Therefore, we decided to quantify RAD51 protein expression. RAD51 is implicated in homologous recombination repair and was reported to be overexpressed in GBM (39). The labeling of RAD51 in cell nuclei of all GBM cell types, in addition to cyclin A immunolabeling ensuring that the counting was performed on cell under S/G_2 phase of the cell cycle, shows that the absence of MKP1 is responsible for a significant delay in the recruitment of the protein 8 h after the irradiation whereas this delay is less pronounced at 12 h. These observations were in agreement with earlier hypothesis: in GBM, MKP1 does play a positive role in DNA strand breaks repair, leading to consequences on cell survival.

In addition to MKP1's role in DNA strand breaks repair in GBM cells, we also wanted to address the possible involvement, direct or indirect, of this nuclear phosphatase in cell survival after irradiation. Therefore, we looked for modifications in the levels of some proteins in response to irradiation when MKP1 is absent or decreased. These proteins have been selected based on their role already demonstrated in this situation in GBM cells or as they have been demonstrated previously to be a substrate for MKP1. This approach appears to be reliable as JNK, a classical MKP1 target, is indeed phosphorylated in irradiated GBM cells depleted of MKP1 activity. The stabilization or slight increase in either PARP1 or MCL1 in irradiated GBM cells when MKP1 is present is original as the stabilization of both proteins after irradiation has never been demonstrated together. MKP1 has already been shown to be able to stabilize PARP1 to mediate cisplatin resistance and to prevent cell death (40). The classical PARP1 role after irradiation is to recruit DNA repair proteins such as RAD51 and stabilizing it indirectly *via* BRCA1 at the site of the break (32). The decrease of PARP1 in irradiated GBM cells depleted for MKP1 could thus explain the delay of RAD51 observed in those cells. It was recently reported that a co-immunoprecipitation of MCL1 and MKP1 in osteosarcoma U2OS cancer cell line had a major impact on cells survival under stress conditions (Jagannathan,V. Thesis, unpublished work). In addition, MCL1 and its short form c-MCL1 can also help to repair double strand breaks by recruiting DNA repair proteins (36) after irradiation and by blocking the cell cycle (41), respectively. The cleaved form (c-MCL1) is generally known for its inhibitory role against the longer form (MCL1), enhancing apoptotic pathways (42). In this study, neither the long form of MCL1 decreased when the c-MCL1 increased in WT cells, nor the survival decreased in those cells after irradiation. This indicates that the c-MCL1 has an important role in the survival of GBM cells after the irradiation. Besides, these forms, especially the cleaved form, decrease or disappear in irradiated GBM cells invalidated for MKP1. This could be a consequence of JNK activity in those cells as the phosphorylation on specific residues of MCL1 due to this kinase is a prerequisite to its degradation (43). All these observed modifications in irradiated GBM cells depleted for MKP1 could thus participate in the increased cleavage of caspase-3 contrary to MKP1-expressing and irradiated GBM cells. This suggests an indirect role of this nuclear phosphatase to the GBM cells survival after irradiation.

Supplementary material

Supplementary data are available at *Carcinogenesis* online.

Funding

The National Fund for Scientific Research (F.N.R.S.) and the Télévie organization, the Special Funds of the University of Liège; an Anti-Cancer Centre near the University of Liège and Léon Frédéricq Grants.

Acknowledgements

M.D. and B.R. would like to thank the GIGA Viral Vectors Platform and the GIGA Imaging Platform (University of Liège, Liège, Belgium) and a special thanks to K.Vieri and F.Giroulle for their technical support.
Conflict of Interest Statement: None declared.

References

1. Lara-Velazquez, M. *et al.* (2017) Advances in brain tumor surgery for glioblastoma in adults. *Brain Sci.*, 7, 1–16.
2. Mallick, S. *et al.* (2016) Management of glioblastoma after recurrence: a changing paradigm. *J. Egypt. Natl. Canc. Inst.*, 28, 199–210.
3. Kroonen, J. *et al.* (2011) Human glioblastoma-initiating cells invade specifically the subventricular zones and olfactory bulbs of mice after striatal injection. *Int. J. Cancer*, 129, 574–585.
4. Singh, S.K. *et al.* (2004) Identification of human brain tumour initiating cells. *Nature*, 432, 396–401.
5. Goffart, N. *et al.* (2015) Adult mouse subventricular zones stimulate glioblastoma stem cells specific invasion through CXCL12/CXCR4 signaling. *Neuro. Oncol.*, 17, 81–94.
6. Goffart, N. *et al.* (2014) Glioblastoma stem cells : new insights in therapeutic strategies. *Future Neurol.*, 9, 1–15.
7. Goffart, N. *et al.* (2017) CXCL12 mediates glioblastoma resistance to radiotherapy in the subventricular zone. *Neuro. Oncol.*, 19, 66–77.
8. Mistry, A.M. *et al.* (2017) Influence of glioblastoma contact with the lateral ventricle on survival: a meta-analysis. *J. Neurooncol.*, 131, 125–133.
9. Chen, L. *et al.* (2015) Glioblastoma recurrence patterns near neural stem cell regions. *Radiother. Oncol.*, 116, 294–300.
10. Chen, L. *et al.* (2013) Increased subventricular zone radiation dose correlates with survival in glioblastoma patients after gross total resection. *Int. J. Radiat. Oncol. Biol. Phys.*, 86, 616–622.
11. Khalifa, J. *et al.* (2017) Subventricular zones: new key targets for glioblastoma treatment. *Radiat. Oncol.*, 12, 67.
12. Achanta, P. *et al.* (2012) Subventricular zone localized irradiation affects the generation of proliferating neural precursor cells and the migration of neuroblasts. *Stem Cells*, 30, 2548–2560.
13. Capilla-Gonzalez, V. *et al.* (2016) Implications of irradiating the subventricular zone stem cell niche. *Stem Cell Res.*, 16, 387–396.
14. Dedobbeleer, M. *et al.* (2017) Phosphatases and solid tumors: focus on glioblastoma initiation, progression and recurrences. *Biochem. J.*, 474, 2903–2924.
15. Wancket, L.M. *et al.* (2012) Mitogen-activated protein kinase phosphatase (MKP)-1 in immunology, physiology, and disease. *Life Sci.*, 90, 237–248.
16. Yu, H. *et al.* (2012) Constitutive expression of MAP kinase phosphatase-1 confers multi-drug resistance in human glioblastoma cells. *Cancer Res. Treat.*, 44, 195–201.
17. Mills, B.N. *et al.* (2017) Expression profiling of the MAP kinase phosphatase family reveals a role for DUSP1 in the glioblastoma stem cell niche. *Cancer Microenviron.*, 10, 57–68.
18. Arrizabalaga, O. *et al.* (2017) High expression of MKP1/DUSP1 counteracts glioma stem cell activity and mediates HDAC inhibitor response. *Oncogenesis*, 6, 401.
19. Seidel, S. (2015) Isolation and culture of primary glioblastoma cells from human tumor specimens. In Rich, I. (ed.) *Stem Cell Protocols. Methods in Molecular Biology (Methods and Protocols)*, Vol. 1235. Humana Press, New York, NY.

20. Verhaak, R.G.W. *et al.* (2010) Integrated genomic analysis identifies clinically relevant subtypes of glioblastoma characterized by abnormalities in PDGFRA, IDH1, EGFR, and NF1. *Cancer Cell*, 17, 98–110.
21. Willems, E. *et al.* (2018) Aurora A plays a dual role in migration and survival of human glioblastoma cells according to the CXCL12 concentration. *Oncogene*, 38, 73–87.
22. Fricker, S.P. *et al.* (2006) Characterization of the molecular pharmacology of AMD3100: a specific antagonist of the G-protein coupled chemokine receptor, CXCR4. *Biochem. Pharmacol.*, 72, 588–596.
23. Slack, D.N. *et al.* (2001) Distinct binding determinants for ERK2/p38alpha and JNK map kinases mediate catalytic activation and substrate selectivity of map kinase phosphatase-1. *J. Biol. Chem.*, 276, 16491–16500.
24. Broome, D.T. *et al.* (2016) Mitogen-activated protein kinase phosphatase-1: function and regulation in bone and related tissues. *Connect. Tissue Res.*, 57, 175–189.
25. Wu, J.J. *et al.* (2005) The noncatalytic amino terminus of mitogen-activated protein kinase phosphatase 1 directs nuclear targeting and serum response element transcriptional regulation. *Mol. Cell. Biol.*, 25, 4792–4803.
26. Yadav, V.N. *et al.* (2016) CXCR4 increases in-vivo glioma perivascular invasion, and reduces radiation induced apoptosis: a genetic knockdown study. *Oncotarget*, 7, 83701–83719.
27. Walters, M.J. *et al.* (2014) Inhibition of CXCR7 extends survival following irradiation of brain tumours in mice and rats. *Br. J. Cancer*, 110, 1179–1188.
28. Flüh, C. *et al.* (2016) Differential expression of CXCR4 and CXCR7 with various stem cell markers in paired human primary and recurrent glioblastomas. *Int. J. Oncol.*, 48, 1408–1416.
29. Candas, D. *et al.* (2014) Mitochondrial MKP1 is a target for therapy-resistant HER2-positive breast cancer cells. *Cancer Res.*, 74, 7498–7509.
30. Sharma, A.K. *et al.* (2015) MKP1 phosphatase mediates G1-specific dephosphorylation of H3Serine10P in response to DNA damage. *Mutat. Res.*, 778, 71–79.
31. Tachon, G. *et al.* (2018) Cell cycle changes after glioblastoma stem cell irradiation: the major role of RAD51. *Int. J. Mol. Sci.*, 19, 3018.
32. Ray Chaudhuri, A. *et al.* (2017) The multifaceted roles of PARP1 in DNA repair and chromatin remodelling. *Nat. Rev. Mol. Cell Biol.*, 18, 610–621.
33. Wu, D.M. *et al.* (2019) MCL1 gene silencing promotes senescence and apoptosis of glioma cells via inhibition of the PI3K/Akt signaling pathway. *IUBMB Life*, 71, 81–92.
34. Morciano, G. *et al.* (2016) Mcl-1 involvement in mitochondrial dynamics is associated with apoptotic cell death. *Mol. Biol. Cell*, 27, 20–34.
35. Zhang, Y. *et al.* (2015) Mcl-1 downregulation sensitizes glioma to bortezomib-induced apoptosis. *Oncol. Rep.*, 33, 2277–2284.
36. Mattoo, A.R. *et al.* (2017) MCL-1 depletion impairs DNA double-Strand break repair and reinitiation of stalled DNA replication forks. *Mol. Cell. Biol.*, 37,
37. Phillips, H.S. *et al.* (2006) Molecular subclasses of high-grade glioma predict prognosis, delineate a pattern of disease progression, and resemble stages in neurogenesis. *Cancer Cell*, 9, 157–173.
38. Stanzani, E. *et al.* (2017) Radioresistance of mesenchymal glioblastoma initiating cells correlates with patient outcome and is associated with activation of inflammatory program. *Oncotarget*, 8, 73640–73653.
39. King, H.O. *et al.* (2017) RAD51 is a selective DNA repair target to radiosensitize glioma stem cells. *Stem Cell Reports*, 8, 125–139.
40. Wang, J. *et al.* (2017) MKP-1 suppresses PARP-1 degradation to mediate cisplatin resistance. *Oncogene*, 36, 5939–5947.
41. Jamil, S. *et al.* (2005) A proteolytic fragment of Mcl-1 exhibits nuclear localization and regulates cell growth by interaction with Cdk1. *Biochem. J.*, 387(Pt 3), 659–667.
42. Bae, J. *et al.* (2000) MCL-1S, a splicing variant of the antiapoptotic BCL-2 family member MCL-1, encodes a proapoptotic protein possessing only the BH3 domain. *J. Biol. Chem.*, 275, 25255–25261.
43. Wang, W. *et al.* (2014) MCL-1 degradation mediated by JNK activation via MEKK1/TAK1-MKK4 contributes to anticancer activity of new tubulin inhibitor MT189. *Mol. Cancer Ther.*, 13, 1480–1491.